Compact, Low-profile and Robust Inversely E-shaped antenna Integrated with EBG Structures for Wearable Application

A. Ashyap, Z.Z. Abidin, S. H. Dahlan, S.M. Shah, S.K. Yee, H.A. Majid, S.A. Qureshi and C.H. See

***Abstract* — A compact and robust inversely E-shaped antenna (IESA) integrated with electromagnetic band-gap (EBG) is presented for wearable applications at 2.4 GHz. The EBG introduced in this paper to shield the antenna from body effects, due to its high natural dielectric. With EBG, the antenna shows good performance under bending and loading human body. The design has overall dimension of 46×46×2.4 mm^3. The integration of antenna with EBG shows an improvement of a gain of 7.8 dBi and bandwidth of 27%. It also reduces the specific absorption rate (SAR) by more than 95.**

Index Terms — EBG, AMC, SAR, wearble textile antennas,

I. INTRODUCTION

Wearable devices are highly desirable to support variety of wearable technologies because of their flexibility, and ease of integration with cloths. Through wearable technologies, wireless human sensing systems can now support a variety of Internet of Things (IoT) applications such as but not limited to monitoring of human vital signs and personal health, smart home, firefighters, tracking, and smartwatches. In this wearable devices, antennas play a vital role in the performance of communication systems for body worn devices. Therefore, several factors to be consider when designing a wearable antenna, such as deformation, loading on body and comfortability of users [1]-[6].

Operating the antennas close proximity to human body effects their performance such as detuning and attenuation of resonant frequency, distortion of the radiation pattern, drop of the efficiency and gain. In addition, mismatches and losses result by human tissue make the design of efficient antennas challenging, especially when it is required to have lightweight, robust, high radiation efficiency and low profile characteristics [7],[8].

Several types of configuration such as substrate integrated waveguide antenna, inverted-F antennas, CPW antenna, microstrip patch antenna, and cavity-backed antenna [9]-[13] have been explored for their suitability as wearable antennas. But these designs carried some drawbacks such large lateral size, narrow bandwidth and high back radiation.

Recently, a huge effort has been devoted to minimize antenna-human interactions. In line with previous research, several designs such as full ground plane, AMC, EBG, MTM, HIS [14]-[19], placed behind the antenna have been proposed to enhance antenna performances whereas reducing the back radiation towards the body. Nevertheless, these structures still electrically large and have a poor FBR.

In this paper, we provide further results from a study of a novel fabric antenna integrated with EBG that was initially outlined in [20]. The overall dimension of the design is 46×46×2.4 mm^3. The design has a novelty of demonstrating the feature of EBG (suppress surface wave) and AMC (in phase) that improve antenna characteristics such as bandwidth, gain, FBR and SAR.

II. DESIGN METHODOLOGY

The optimized novel presented inversely E-shaped antenna (IESA) was briefly reported in [20]. A specific slot is introduced in the radiating patch of the microstrip antenna forming a novel inversely E-shaped design. The slots meandered the excited patch surface current path causes the resonant frequency of the antenna to decrease, which corresponds to a reduction in antenna size. The detail design scheme and the study of the IESA structure are clearly shown in [11].

The novel structure of the EBG unit cell was initially started with square loop. The square loop was tuned to yield a 0^0 reflection phase at 2.4 GHz with overall dimension of 32×32×0.7 mm^3 as depicted in Fig.1 (a). The square loop structure able only to show the in-phase feature, due to the absent of via that result of shifting the band-gap to higher frequencies.

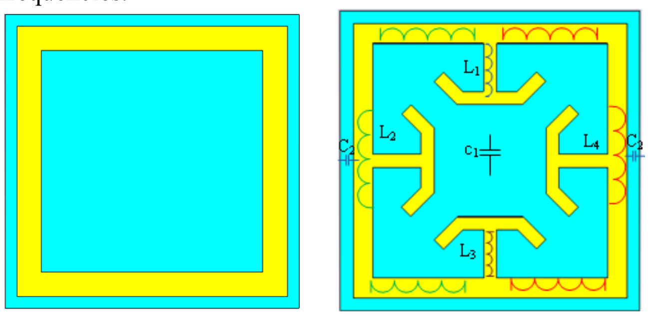

(a) (b)

Fig.1.EBG unit cell (a) conventional square loop, and (b) Proposed design

Removing Via from EBG makes the design fabrication process easier but the feature of band-gap disappear. To have the feature of band-gap without having Via, four T-shaped was added to the square loop forming a novel shape as depicted in Fig.1 (b). These T-shaped have increased the effective inductance which demonstrated the features of EBG/AMC and reduced the size by 51.42% compared to the conventional square loop design.

The proposed EBG unit cell was examined by two methods [21]. The reflection phase that shows the feature of in-phase crossing 0^0 at 2.4 GHz which mimic the characteristic of PMC that does not exist in nature. The band-gap that covers from 2.18 GHz to 2.8 GHz which indicates the suppression of surface wave within this range. The result of reflection phase of both the conventional square loop and the proposed design are illustrated in Fig. 2(a) whereas the bandgap of proposed design is depicted in Fig. 2(b).

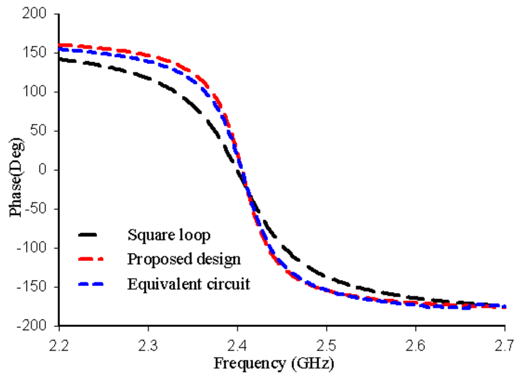

(a)

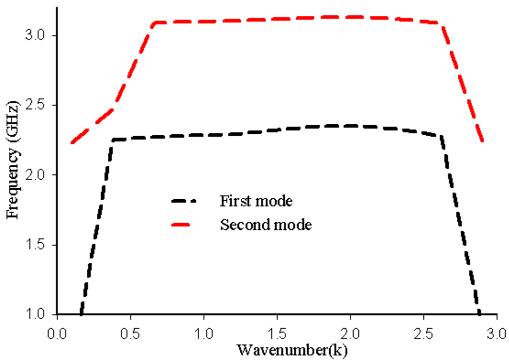

(b)

Fig.2. (a) reflection phase, and (b) Band-gap

The physical structure of the proposed EBG unit cell is modelled as equivalent circuit as depicted in Fig 3. The inductances are due to the strip lines while the capacitances are due to the gap between the neighboring unit cells and the gap between the strips. The values of inductance and capacitance can be determined based on the following equations [16]:

$$L = \ell\frac{\mu_0}{4\pi}ln\left\{1+\frac{32h^2}{w^2}\left[1+\sqrt{1+\left(\frac{\pi w^2}{8h^2}\right)^2}\right]\right\} \quad (1)$$

where ℓ and w are the length and width of the strip lines, and h is the substrate height.

$$C = \frac{W\varepsilon_0(1+\varepsilon_r)}{\pi}cosh^{-1}\left(\frac{W+g}{g}\right) \quad (2)$$

where W is width of patch, and g is the gap

$$L_d = \mu_0 h \quad (3)$$

Fig.2 (a) presents the comparison of reflection phase attained from the equivalent circuit and the full wave. It is observed that the result in good agreement.

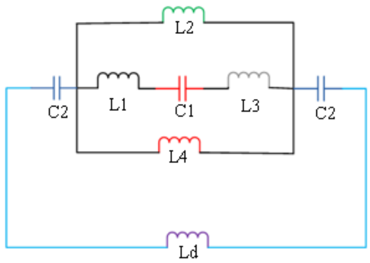

Fig.3. Equivalent circuit model of proposed design

III. EXPERIMENTAL INVESTIGATIONS AND ANALYSES

The IESA is positioned on top of the EBGs as shown in Fig. 4. Foam with thickness of 1 mm separates the IESA and EBGs to diminish the mismatch as well as to avoid any short circuit. It was shown in [19] that the S_{11} and radiation pattern of the presented antenna with EBG demonstrate a superior performance with a bandwidth of 27 % (measured), the gain of 7.8 dBi (simulated) and the FBR of 15.5 dB (measured).


(a) (b)

Fig.4.Fabricated antenna with EBG structure (a) Front view and (b) Back view

IV. FURTHER INVESTIGATION AND DISCUSSION

A. Bending Assessment

In more than a few applications, the flexible antennas are expected to be bend or load to human body surfaces during operation. Hence, before studying the human body tissue loading influence, an examination on the performance of the proposed design under several degrees of structural deformation in free space is demanded, to confirm its reliability. Two different orientations have been considered: x-axis, and y-axis, and experimentally tested. The bending was conducted with several diameters (d) of 70 mm 80 mm, 100 mm, and 140 mm. These diameters corresponds to different size of human legs and arms.

The experimental result depicted in Fig.5. The results reveal that the shift of the resonant frequency of both orientations are insignificant, since the desired band still below -10 dB even at extremely degree of bending.

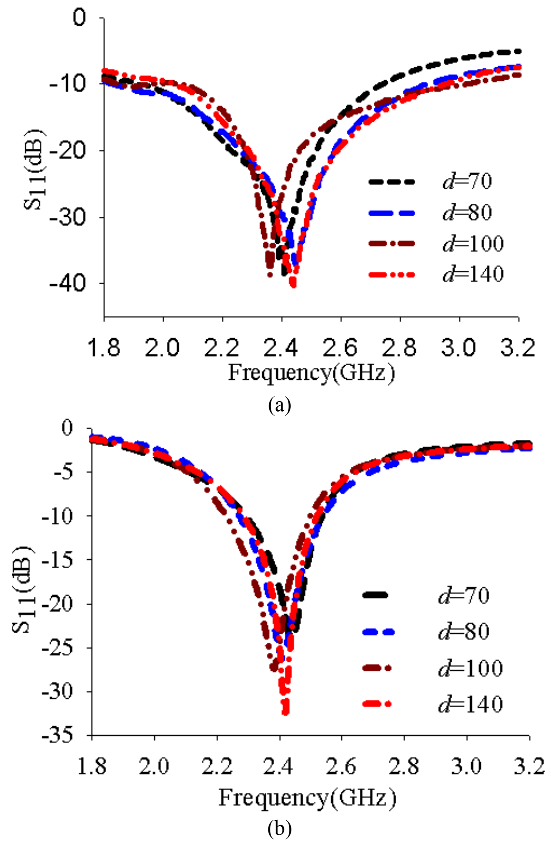

Fig.5. S_{11} measurement of the integrated antenna with EBG under bending at the (a) y-axis, and (b) x-axis.

The radiation pattern under bending was also experimentally carried out at diameter of 140 mm as depicted in Fig.6. The obtained result was compared with measured in free space. The result is comparable with minor effects that could due non-ideal uniformity of the bending diameters across the structure.

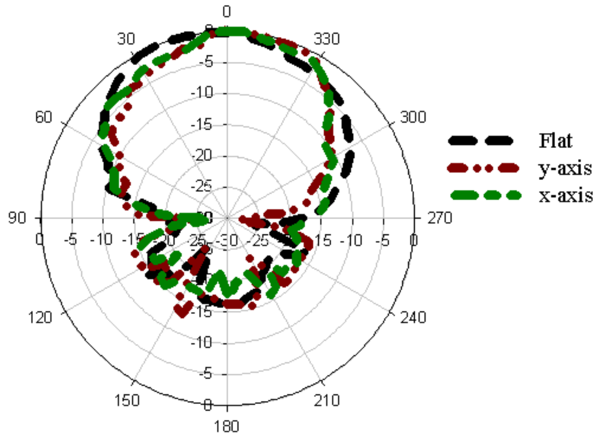

Fig.6. Radiation pattern measurement under bending at diameter 140 mm along y-axis and x-axis

B. Effects of Human Tissues Loading

The EBG used in this design to shield the antenna from the body effect. Hence the resonant frequency will not detune and attenuate. To valid this, the design was experimentally examined by placing the design on chest and back of volunteer male. The results is depicted in Fig.7. It is seen that the S_{11} is stable and cover the desired band. This indicates that the EBG shield the antenna from the body that has high neutral dielectric which detune the resonant frequency.

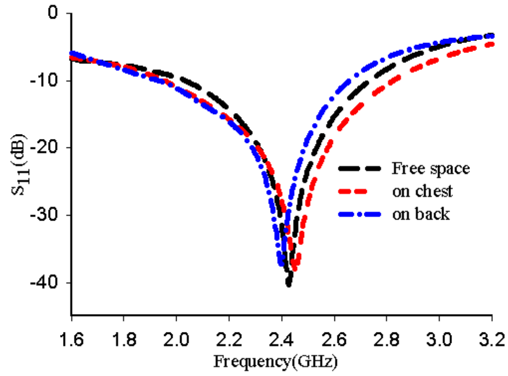

Fig.7. S_{11} measurement of the integrated antenna with EBG positioned on chest and back of real body

The performance radiation patterns of the antenna alone and antenna with EBG when the design placed on the chest were numerically tested and compared with case of free space. The result shows that when the antenna is alone the body absorbed high radiation compared to free space as seen in Fig.8, whereas when the antenna with EBG the radiation pattern is comparable indicting of less radiation absorbed by body as seen in Fig.9. This shows the useful of introducing EBG in the antenna design.

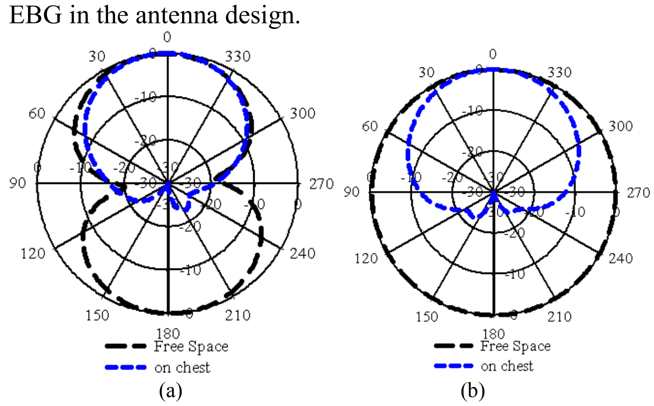

Fig.8. Simulated radiation patterns of the antenna alone on chest model (a) E-plane, and (b) H-plane.

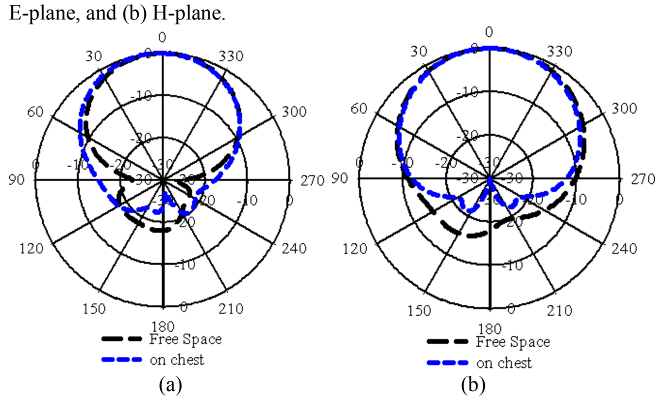

Fig.9. Simulated radiation patterns of the antenna with EBG on chest model (a) E-plane, and (b) H-plane.

C. SAR Assessment

To find the amount of electromagnetic radiation captured by the tissues in the body, assessment of the SAR becomes essential to confirm the safety level is below the standards. Based on the guideline given by the FCC, the SAR values should be less than 1.6 W/kg averaged over 1 g of human tissues [19].

TABLE I
SAR VALUES WITH AND WITHOUT EBG ON CHEST

Different distances between the design model	Antenna a lone	Antenna with EBG
0	7.42	0.093
1	6.48	0.032
3	5.16	0.02

A multi-layer model developed to represent the chest for SAR analysis. The model have four layers which are skin, bone, fat, and muscle and have a dimension of 150×150×40 mm^3. The data and thickness of each layer is taken from [19]. 100 mW was selected as input power. The analysis is carried out using IEEE C95.1 standard provided in the CST. The design was placed with different distances from the model to study the influence on the SAR levels. Fig.10. displays the simulated SAR at 1 mm away from the chest .Furthermore, the SAR value at 2.4 GHz of the antenna with and without EBG at 1 g is summarized in Table I. the result indicates that when the antenna is alone the SAR levels exceed the standards, while when EBG was adding to the antenna the SAR values reduces by more than 95%. As a result, it is obvious from the SAR levels that the EBG is operating well as a PMC at the higher frequencies.

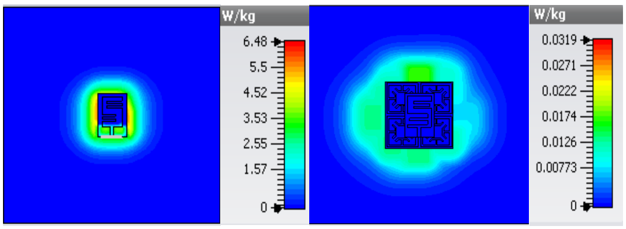

(a) (b)

Fig.10. SAR levels at 1 mm far from the chest (a) antenna alone,(b) and antenna with EBG

V. CONCLUSION

A robust and compact fully fabric antenna incorporated with EBG for wearable application is effectively designed and experimentally tested. The EBG in this design shield the antenna from the body and improved the performance of the antenna compared to the case without EBG. The proposed design shows good performance under deformation and loading of the body. Furthermore it achieves a gain of 7.8 dBi and a bandwidth of 27%, at the desired band and reduced the radiation into the body by over 15 dB. Besides that, it reduces the SAR values by more than 95% compared to antenna alone.

REFERENCES

[1] A. Y. I. Ashyap, Z. Z. Abidin, S. H. Dahlan, H. A. Majid, and F. C. Seman, "A Compact Wearable Antenna Using EBG for Smart-Watch Applications," *in 2018 Asia-Pacific Microwave Conference (APMC)*, 2018, pp. 1477–1479.

[2] N. H. Abd Rahman, Y. Yamada, and M. S. Amin Nordin, "Analysis on the Effects of the Human Body on the Performance of Electro-Textile Antennas for Wearable Monitoring and Tracking Application," *Materials (Basel).*, vol. 12, no. 10, p. 1636, May 2019.

[3] A. Y. I. Ashap, Z Z Abidin, S H Dahlan, H A Majid, S K Yee, Gameel Saleh, and Norun Abdul Malek, "Flexible Wearable Antenna on Electromagnetic Band Gap using PDMS substrate," *TELKOMNIKA* ,vol. 15, no. 3, pp. 9–12, 2017.

[4] F. C. Seman, F. Ramadhan, N. S. Ishak, R. Yuwono, Z. Z. Abidin, S. H. Dahlan, S. M. Shah, and A. Y. I. Ashyap, "Performance Evaluation of a Star-Shaped Patch Antenna on Polyimide Film Under Various Bending Conditions," *Progress In Electromagnetics Research Letters*, Vol. 85, 125-130, 2019.

[5] A. Y. I. Ashyap *et al.*, "A wearable antenna based on fabric materials with circular polarization for Body-centric wireless communications," *Indones. J. Electr. Eng. Comput. Sci.*, vol. 18, no. 1, p. 335, Apr. 2020.

[6] A. Y. I. Ashyap, W. N. N. W. Marzudi, Z. Z. Abidin, S. H. Dahlan, H. A. Majid, and M. R. Kamaruddin, "Antenna incorporated with Electromagnetic Bandgap (EBG) for wearable application at 2.4 GHz wireless bands," *in 2016 IEEE Asia-Pacific Conference on Applied Electromagnetics (APACE)*, 2016, no. December, pp. 217–221.

[7] A. Al-Sehemi, A. Al-Ghamdi, N. Dishovsky, N. Atanasov, and G. Atanasova, "Miniaturized Wearable Antennas with Improved Radiation Efficiency Using Magneto-dielectric Composites," *IETE J. Res.*, vol. 0, no. 0, pp. 1–11, Jul. 2019.

[8] A. Y. I. Ashyap, Z. Z. Abidin, S. H. Dahlan, H. A. Majid, and F. C. Seman, "A Compact Wearable Antenna Using EBG for Smart-Watch Applications," in *2018 Asia-Pacific Microwave Conference (APMC)*, 2018, vol. 2018-Novem, pp. 1477–1479.

[9] R. Moro, S. Agneessens, H. Rogier, and M. Bozzi, "Wearable textile antenna in substrate integrated waveguide technology," *Electron. Lett.*, vol. 48, no. 16, pp. 985–986, Aug. 2012.

[10] Z. Muhammad, S. M. Shah, Z. Z. Abidin, A. Y. I. Asyhap, S. M. Mustam, and Y. Ma, "CPW-fed wearable antenna at 2.4 GHz ISM band," *AIP Conference Proceedings 2017*,vol. 1883, no. 1, p. 020003.

[11] A. Y. I. Ashyap, Z. Z. Abidin, S. H. Dahlan, H. A. Majid, Waddah. A. M. A, M. R. Kamarudin, George Adeyinka Oguntala, Raed A. Abd-Alhameed, James M Noras, "Inverted E-Shaped Wearable Textile Antenna for Medical Applications," *IEEE Access*, vol. PP, no. c, pp. 1–1, 2018.

[12] P. J. Soh, G. A. E. Vandenbosch, S. L. Ooi, and N. H. M. Rais, "Design of a broadband all-textile slotted PIFA," *IEEE Trans. Antennas Propag.*, vol. 60, no. 1, pp. 379–384, Jan. 2012.

[13] H. Memarzadeh-Tehran, R. Abhari, and M. Niayesh, "A cavity-backed antenna loaded with complimentary split ring resonators," *AEU - Int. J. Electron. Commun.*, vol. 70, no. 7, pp. 928–935, Jul. 2016.

[14] A. Y. I. Ashyap, Z. Zainal Abidin, S. H. Dahlan, H. A. Majid, and G. Saleh, "Metamaterial inspired fabric antenna for wearable applications," *Int. J. RF Microw. Comput. Eng.*, vol. 29, no. 3, p. e21640, Mar. 2019.

[15] Z. Jiang, D. E. Brocker, P. E. Sieber, and D. H. Werner, "A compact, low-profile metasurface-enabled antenna for wearable medical body-area network devices," *IEEE Trans. Antennas Propag.*, vol. 62, no. 8, pp. 4021–4030, Aug. 2014.

[16] S. Yan, L. A. Y. Poffelie, P. J. Soh, Xuezhi Zheng, and G. A. E. Vandenbosch, "On-body performance of wearable UWB textile antenna with full ground plane," in *2016 10th European Conference on Antennas and Propagation (EuCAP)*, 2016, pp. 1–4.

[17] A. Y. I. Ashyap, Z. Z. Abidin, S. H. Dahlan, H. A. Majid, M. R. Kamarudin, "Highly Efficient Wearable CPW Antenna Enabled by EBG-FSS Structure for Medical Body Area Network Applications," *IEEE Access*, vol. 6, pp. 77529–77541, 2018.

[18] A. Kamalaveni and M. Ganesh Madhan, "A compact TRM antenna with high impedance surface for SAR reduction at 1800 MHz," *AEU - Int. J. Electron. Commun.*, vol. 70, no. 9, pp. 1192–1198, Sep. 2016.

[19] A. Y. I. Ashyap *et al.*, "Robust and Efficient Integrated Antenna With EBG-DGS Enabled Wide Bandwidth for Wearable Medical Device Applications," *IEEE Access*, vol. 8, pp. 56346–56358, 2020.

[20] A. Y. I. Ashyap, Z. Z. Abidin, S. H. Dahlan, H. A. Majid, S.Shah, M. R. Kamarudin and A.Alomainy, "Compact and Low-profile Textile EBG-based Antenna for Wearable Medical Applications," *IEEE Antennas Wirel. Propag. Lett.*, vol. 1225, no. c, pp. 1–1, 2017.

[21] A. Y. I. Ashyap *et al.*, "An Overview of Electromagnetic Band-Gap Integrated Wearable Antennas," *IEEE Access*, vol. 8, pp. 7641–7658, 2020.